

# GAS FLOW THROUGH A SLIT INTO VACUUM IN A WIDE RANGE OF RAREFACTIONS

*O. Sazhin*\*

*Ural State University  
620083, Ekaterinburg, Russia*

Received February 7, 2008

Gas flow through a two-dimensional slit into vacuum is investigated by a direct simulation Monte Carlo method. Results for mass flow rate are obtained as a function of the rarefaction parameter, which is inversely proportional to Knudsen number. The distributions of density, temperature and mass velocity, and streamlines are presented. In the free molecular flow regime and in the hydrodynamic limit, our results agree with theoretical asymptotes, and in the transition regime, they compare well with numerical simulations by other authors.

PACS: 47.60.Dx, 47.61.Fg

## 1. INTRODUCTION

The problem of gas flow through capillaries is classical. Starting with Knudsen, much effort has been invested into it, theoretical as well as experimental [1]. From the theoretical standpoint, it is particularly interesting in that it can give rise to all flow regimes, from free molecular flow to hydrodynamic flow. Recently, applications of this gas-dynamic problem also have been boosted by rapid developments of industrial technologies using micro- and nano-size elements and, in particular, micro- and nano-electromechanical systems (MEMS/NEMS; see, e.g., [2]).

Indeed, the size of micro- and nano-electromechanical systems is the reason that they work in regimes that differ significantly from working regimes of similar macroscopic devices. A very important consequence of their extremely small scale is that the usual treatment of gas flow in them as continuous media with macroscopic state parameters varying smoothly in space and time becomes impossible. This effect could be quantified by using the Knudsen number  $Kn$  defined as the ratio of the mean free path of gas molecules to the characteristic size of the system. For example, at standard room temperature, normal atmospheric pressure, and system size of 1 micron, the Knudsen number is 0.07. But the continuous media approach to gas flow breaks at Knudsen numbers above about 0.01. If such

a device is meant to be used at high altitudes (i.e., aerospace industry), at low pressures (vacuum technologies) or has size much less than 1 micron, the effect is significantly more pronounced. In addition, in micro- and nano-electromechanical systems, the scattering of gas molecules on the surface, and therefore the structure of the surface and accommodation properties of gas molecules, become increasingly important. Sometimes, geometric sizes of the working elements are such that the structure of the surface and interfaces is crucial. Depending on application, MEMS/NEMS could have surfaces ranging from very smooth silicon to quite rough technical surface.

In reality, interaction of gas flow with surfaces of micro- and nano-electromechanical systems could differ significantly from the standard theoretical approach used in most engineering applications, where perfect accommodation of energy and momentum of gas molecules by the surface is assumed and the corresponding accommodation coefficients are set to unity. Relatively recently, it was shown in experiments [3] that the accommodation coefficient for tangential momentum on an atomically clean surface can be as low as of 0.7, which leads to a 65 % increase in the gas flow through the capillary compared to the theoretical calculations that use the perfect accommodation assumption. Nonperfect accommodation of energy has an even stronger effect. By varying chemical composition of the surface, the corresponding accommodation

---

\*E-mail: oleg.sazhin@uralmail.com

coefficient can be lowered to a dramatically small magnitude of the order of several hundredths, which would have a huge impact on heat transfer in MEMS/NEMS. Another important factor that changes heat transfer behavior is the ratio of the surface area to volume, evidently very different in macro- and microdevices.

All these factors need to be taken into account to model micro- and nano-electromechanical systems correctly. One possible way is to use methods of kinetic gas theory based on the famous integrodifferential Boltzmann equation for the molecular distribution function. To model gas flow through long capillaries, the linearized Boltzmann equation is frequently used [4]. However, gas flow through short capillaries caused by a large difference in pressure becomes essentially nonequilibrium, and therefore much more complicated nonlinear kinetic equations should be used.

An alternative and much more flexible way of studying gas flow is the direct simulation Monte Carlo method [5], which has shown to be an effective tool for problems of gas dynamics for all flow regimes, from hydrodynamic flow, for which the continuous media approximation works so well, to free molecular flow. The direct simulation Monte Carlo method allows taking many different factors into account, such as nonequilibrium and complex geometric configuration of the system, and using different boundary conditions, models of surface structure and assumptions about molecular interactions. An additional justification for using numerical simulations in developing MEMS/NEMS is that carrying out extensive experiments in design phase is extremely difficult and economically infeasible. In fact, doing this sometimes requires creating even more complex gauges that would allow measuring flows, for example, inside MEMS/NEMS. Very often, developing them becomes more of an empirical process. Therefore, there is a need to develop and implement methods of numerical modeling of gas flow processes in micro- and nano-electromechanical systems. These methods should be capable, in the first place, to produce preliminary crude data on main characteristics of a system, model and optimize working regimes, compare different designs, and so on.

By a “slit”, we mean an infinitesimally thin capillary with a rectangular cross section. Overall, there has not been much either experimental or theoretical research done on rarefied gas flow into vacuum through a slit.

The first relatively complete experimental study of gas flow through an orifice (infinitesimally thin capillary with cylindrical cross section) was done by Liepmann [6]. He also argued theoretically that for a two-dimensional problem in the hydrodynamic limit and

large pressure drop, a somewhat greater mass flow rate through a slit than through an orifice should be expected. However, his own conclusion was that the difference should be quite small.

Most theoretical papers on gas flow through a slit are based on the assumption that the flow is caused by a small difference in pressure. In particular, the system of integral equations for gas velocity, density, and temperature derived from the linearized Boltzmann–Krook–Welanders equation with the diffuse reflection boundary condition was solved numerically in [7] by a Neumann series expansion. As a result, the gas density, temperature, flow velocity distributions, and mass flow rates for different Knudsen numbers were obtained.

In Ref. [8], rarefied gas flow between two containers divided by a short “channel” — a rectangular slit with the parameters  $l/h = 0.05$  and  $w/h = 20$ , where  $l$  is the length,  $w$  is the width, and  $h$  is the height of the slit — was studied experimentally for Knudsen numbers from 0.0521 to 2.521. Mass flow rate measurements were done for values of pressure difference between the containers of 3, 6, 10, and 15 times.

Numerical modeling of rarefied gas flow through a slit was done in [9,10]. In Ref. [9], two approaches were used to analyze gas flow from one container into another through a slit: an approach based on numerical solution of the equations of gas dynamics using the method of finite differences, and the direct simulation Monte Carlo approach. The problem was solved in two dimensions for two different values of the ratio of pressures in the containers: a large value corresponding to flow into vacuum and the pressures ratio equal to 2. In the direct simulation Monte Carlo approach, the variable hard-sphere model for Argon was used to describe interactions between gas molecules, and a no-time-counter scheme to model collision relaxation. At the surface, diffuse scattering was assumed. The size of the computation domain was  $5 \times 2.5$  slit heights both upstream and downstream for simulation at any Knudsen number. The mass flow rate, density and temperature distribution, and mass velocity along the center line of the slit from the free molecular regime to the transition regime ( $Kn = 0.05$ ) were analyzed. For the free molecular flow regime, the results were compared with analytic expressions. Similar computations were done in [10] for the hard-sphere model for the pressures ratios 2, 10, and 50 and Knudsen numbers 0.2, 1, and 10. The size of the computation domain was chosen in [10] as approximately ten local mean free paths upstream and three to five downstream.

Thus, in spite of great practical importance, gas flow through a slit into vacuum has not been investi-

gated in detail. Numerical studies pay little attention to the accuracy of computations and justification of model parameters, in particular, the size of the computation domain. There is no data on the mass flow rate in a wide range of rarefactions.

In this paper, we compute the mass flow rate through a slit into vacuum in a wide range of rarefactions and study the flow field using a direct simulation Monte Carlo method.

## 2. STATEMENT OF THE PROBLEM AND DEFINITIONS

We take a system consisting of two large containers connected by a slit. We assume the size of the containers large enough to consider the length of the slit equal to zero,  $l = 0$ . Far from the slit, the upstream container contains an equilibrium monatomic gas at a pressure  $P_1$  and a temperature  $T_1$ . The pressure in the downstream container,  $P_2$ , is so small (compared to  $P_1$ ) that we can assume  $P_2 = 0$ . If the width of the slit is much greater than its height,  $w \gg h$ , we can reduce the problem to only two dimensions.

Let  $Q$  be the mass flow rate through the slit. We are primarily interested in the mass flow rate normalized by its value  $Q^* = Q/Q_{fm}$  in the free molecular flow regime as a function of the rarefaction parameter

$$\delta = \frac{hP_1}{\mu_1 v_1} = \frac{\sqrt{\pi}}{2\text{Kn}}, \quad (1)$$

where  $\mu_1$  and  $v_1$  are respectively the gas viscosity and the most probable molecular velocity at the reference temperature  $T_1$ . As we can see, the rarefaction parameter  $\delta$  is inversely proportional to the Knudsen number  $\text{Kn}$ , defined for the slit as  $\text{Kn} = \lambda_1/h$ , where  $\lambda_1$  is the mean free path of gas molecules in the upstream container far from the slit.

In the free molecular flow regime,  $\delta = 0$  and the mass flow rate through a two-dimensional slit can be calculated analytically as [4]

$$Q_{fm} = \frac{h}{\sqrt{\pi} v_1} P_1. \quad (2)$$

In the hydrodynamic flow limit, when  $\delta \gg 1$ , the normalized mass flow rate through an ideal nozzle also can be calculated analytically using Euler's equation to be

$$Q^* = \sqrt{2\pi\gamma} \left( \frac{2}{1+\gamma} \right)^{(1+\gamma)/2(1-\gamma)}, \quad (3)$$

where  $\gamma$  is the specific heat ratio ( $\gamma = 5/3$  for monatomic gas). The mass flow through a nonideal

nozzle as a slit can be obtained by multiplying the mass flow rate through an ideal nozzle by the discharge coefficient. A typical value of the discharge coefficient for a two-dimensional slit is 0.85 [6]. Thus, the normalized mass flow rate  $Q^*$  for a monatomic gas through a slit in the hydrodynamic limit should be approximately 1.55.

## 3. THE DIRECT SIMULATION MONTE CARLO METHOD

As is well known, the essence of Monte Carlo methods is to describe a physical system by means of a stochastic process and then estimate various properties of the system as the corresponding mathematical expectations. For rarefied gas dynamics, the stochastic process is the evolution (motion and collisions) of a large number  $N$  of model particles, each of which represents  $F_N = nV/N$  of the real gas molecules, where  $n$  is the gas density and  $V$  is the volume of the system.

There are exact and approximate Monte Carlo schemes. Exact schemes require that after each collision in a system of  $N$  model particles, each of them travels a distance proportional to the time between two consecutive collisions. Such schemes are very computationally intense and time-consuming, and require considerable resources. Therefore, we limited ourselves to using an approximate scheme. In approximate schemes, particle motion and collisions are divided onto time steps  $\Delta t$  that are smaller than the mean time between two collisions  $t_1 = \lambda_1/v_1$ , and are processed independently. In other words, the process of motion and collision of gas molecules is split into two consecutive independent processes, free molecular motion and a spatially homogenous collision relaxation. This speeds up simulations considerably [11]. However, the exact scheme sometimes remains the only possibility, for example, when there are no clear criteria for identifying the time step  $\Delta t$ .

Modeling free molecular motion in systems of simple geometry is relatively easy. The major difficulty in implementing an approximate scheme is therefore to simulate collision relaxation. One way to do it is to divide the modeled space into small cells with the cell size chosen such that gas flow parameters change from cell to cell very little. All cells taken together form a spatial grid on which the simulation is run.

We used a two-level regular grid with different cell sizes at each level (Fig. 1). The minimum cell size on the grid was set to be of the order of or smaller than the mean free path  $\lambda_1$  of gas molecules in equilibrium gas at a pressure  $P_1$  and temperature  $T_1$  (as far from the slit

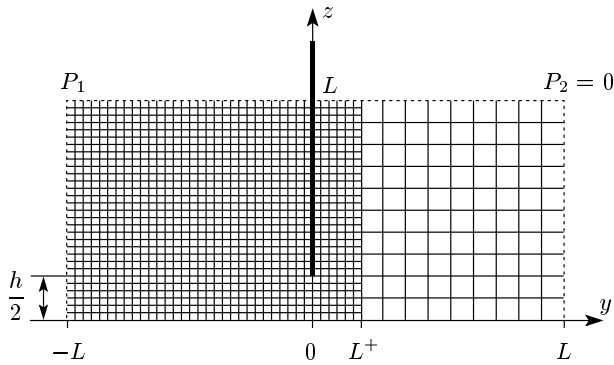


Fig. 1. Model geometry and the computation grid

in the upstream container). As gas flows through the slit into vacuum, its density rapidly decreases. Therefore, in the immediate vicinity of the slit, where the flow state parameters change very rapidly, the free path of gas molecules in this region becomes significantly larger than the cell size (usually, by a factor of 1.5–2). The bold line in Fig. 1 is a part of the slit wall. As shown in the Figure, the second level of the grid begins at some distance  $L^+$  from the slit. It is also natural to assume that the flow is symmetric, and hence placing a mirror boundary at the center line of the slit allows modeling only half of the space directly, which considerably reduces the computation time.

Initially, all particles are placed in the upstream container and obey the Maxwell distribution at the temperature  $T_1$ . Then the particle free motion (i) and collisions (ii) during each time interval  $\Delta t$  are simulated independently.

(i) All molecules in the flow field are displaced by distances determined by their instantaneous velocity and the length of the time interval  $\Delta t$ . If a particle leaves the computation area during this time interval, it is considered lost and is tracked no more (deleted from the system). If a molecule hits a boundary, its velocity changes according to the imposed boundary conditions. Each particle that crosses the slit contributes to the mass flow rate, which is computed as  $N_1 - N_2$ , where  $N_1$  is the number of particles passed through the slit from the upstream container downstream, and  $N_2$  is the number of particles that cross the slit upstream. During the same time interval, new particles that enter the computation area are generated. This occurs at the outer edge of the computation area in the upstream container, and the number and velocities of new particles obey the distribution function for molecules crossing a fixed plane in equilibrium gas at the pressure  $P_1$  and temperature  $T_1$ .

(ii) Collisions between molecules are modeled for

each cell separately. In other words, only particles from the same cell are allowed to collide because they are assumed to be nearest neighbors of one another. However, it is quite possible that for a particle close to a cell boundary, actual nearest neighbors are not the particles in the same cell that happen to be at the other end of it but particles in an adjacent cell. To account for this and ensure that only closest particles collide, each cell was divided into subcells and only collisions for particles in the same subcell were considered to occur. The minimum number of subcells was 9. New velocities of particles after collision are computed from the momentum and energy conservation laws.

It is important to note that the length of the time interval  $\Delta t$  should not only be less than the mean time between two collisions  $t_1$ , but also not greater than the average time a particle spends in one cell.

To simulate collisions, we used the homogenous majorant frequency scheme with consecutive sorting of cells introduced in [12]. As indicated in [12], a necessary condition for its applicability is that the number of collisions during a single time step  $\Delta t$  must be large enough. Another technique widely used in direct simulation Monte Carlo method is the no-time-counter scheme. However, it is believed that being at the same level of computational complexity, the majorant frequency scheme requires fewer particles in the model cell to obtain the collision frequency correctly [13].

A major problem in simulating gas flow into vacuum is that gas densities upstream and downstream the slit differ by orders of magnitude. Because the number of particles in a cell is directly related to the gas density (unless special procedures are used), the number of particles in cells on different sides of the slit could be very different. In particular, a dangerous situation is possible when there are no particles in cells far from the slit downstream, because it may deteriorate the accuracy of simulations.

To overcome this problem and increase the number of particles in the immediate vicinity of the slit in the downstream container (in the region from 0 to  $L^+$ ), we used the weight-factor plane procedure. When particles cross a plane with weight factor 2 going downstream, their number doubles, and when they cross the plane going upstream, their number halves. Clearly, the representation  $F_N$  changes in the inverse proportion. In our simulations, at least 4 weight planes were used, e.g.,  $Y = 0, 0.5h, h, 1.5h$  (see Fig. 1), which corresponds to a 16-fold increase in the number of model particles if they cross all four planes. Using several planes with weight factor 2 allows avoiding a dangerous side effect of having many clone particles (i.e., particles with the

same position and velocity) if only one plane with a high weight factor is used instead.

Position of the second level of the grid  $L^+$  was chosen so as to ensure a density decrease of 8–10 times before particles reach it. In most simulations, we used  $L^+ = 3h$ . Linear size of the cells at the second level was 3 times larger than at the first level, which leads to a 9-fold increase in the number of particles per cell between  $L^+$  and  $L$ .

Altogether, using a nonhomogeneous grid and weight factor planes enables us to achieve a close-to-uniform number of model particles per cell throughout the computation region, which should increase the accuracy of simulations.

#### 4. ERROR ANALYSIS

Produced by a numerical and simulational approach, the results of direct simulation Monte Carlo method are obviously not free of error caused by the statistical nature of the method and approximations made in the process: only a limited number of simulated model particles, each representing a large number of gas molecules, is used, simulations are only run in a finite area close to the slit, continuum space is discretized using a finite space grid, and, finally, the particle free motion and collisions are artificially separated. Therefore, each of these approximations should be treated separately, and the cell and simulation area size, the number of model particles in the cell, and the time interval used in simulations should be analyzed depending on the individual problem basis. Generally, however, we should expect the best results to be obtained using the maximum possible number of model particles and simulation area size, and as small time step and cell size as possible.

When used to model motion and collisions of gas molecules, the direct simulation Monte Carlo method is adequate to the physical nature of molecular transport and can be regarded as a numerical experiment. As in any physical experiment, one can specify two types of errors in this method, a random error that is caused by the statistical nature of the method and depends on the number of time steps (or samples) simulated, and a systematic error that depends on the cell size, the time step length, the number of model particles in a cell, and the simulation area size.

The random error can be greatly reduced by processing a large number of samples. Moreover, the number of samples needed to achieve any required level of random error can be estimated analytically. As well-

known, statistical fluctuations in the results of direct simulation Monte Carlo method are inversely proportional to the square root of the sample size [5]. Fluctuations in the number of particles  $N_1$  coming through the slit downstream can be estimated as  $\sqrt{N_1}$ , and fluctuations in the number of particles coming through the slit upstream,  $N_2$ , are similarly estimated as  $\sqrt{N_2}$ . Because the mass flow through the slit is  $N_1 - N_2$ , the upper and lower estimates for the mass flow are

$$\left(N_1 \pm \sqrt{N_1}\right) - \left(N_2 \mp \sqrt{N_2}\right).$$

Normalizing by the mass flow rate, we obtain

$$1 \pm \frac{\sqrt{N_1} + \sqrt{N_2}}{N_1 - N_2}.$$

We now formulate the condition for random error as follows: we run samples until the inequality

$$\frac{\sqrt{N_1} + \sqrt{N_2}}{N_1 - N_2} < 0.001 \quad (4)$$

is satisfied. Then the random part of error is of the order of 0.1 %.

The systematic part of error is quite remarkable in that if we know where it comes from, we can take it into account and directly correct the results of experiments/simulation for it to reduce its influence to negligible levels (that is, much lower than the random part of simulation error). In direct simulation Monte Carlo method, the systematic error dependence on the parameters of simulations very rapidly becomes asymptotic and does not change the results much when the corresponding parameter of simulations (for example, the cell size) is improved.

Figure 2a shows the dependence of the mass flow rate through the slit on the cell size  $\Delta y (= \Delta z)$  in units of the mean free path  $\lambda_1$  for different sizes  $L$  of the computation domain in the case  $\delta = 1$ . The bars at each data point here and in the following figures show the level of random error. Clearly, the results show that the cell size required to exclude the systematic error depends strongly on  $L$ . For small domain sizes, we should use smaller cells. Besides a dependence on the computation domain size, the optimum for reducing the systematic error clearly depends on the degree of rarefaction  $\delta$ . For large  $\delta$ , the cell size can even exceed the mean free path  $\lambda_1$ . The reason for this is that in this case the cell size is already small enough to have the flow parameters change within one cell very little. Therefore, it has not to be reduced further down to  $\lambda_1$ . Alternatively, dividing into subcells in some cases also

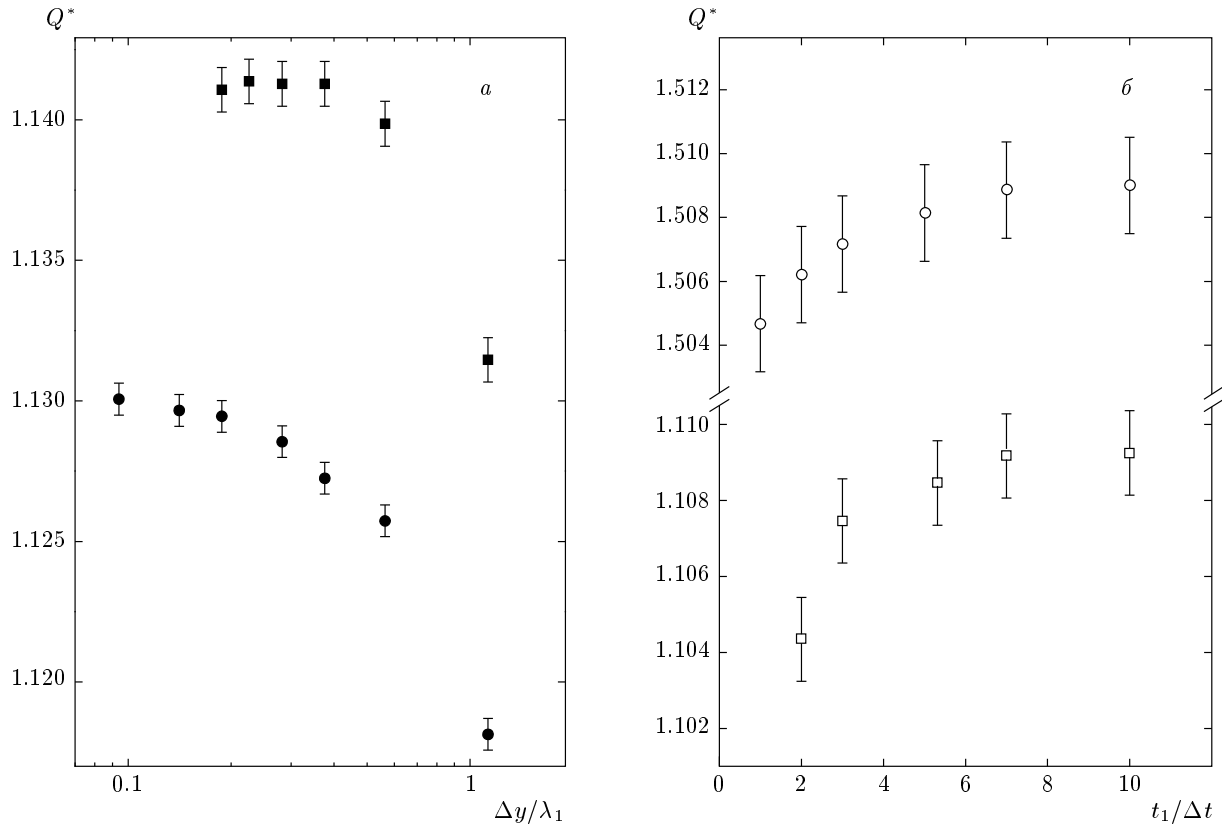


**Fig. 2.** Dependence of the mass flow rate  $Q^*$  through the slit on (a) the dimensionless cell size  $\Delta y/\lambda_1$  for different computation domain sizes  $L = 10h$  ( $\bullet$ ) and  $25h$  ( $\blacksquare$ ) for  $\delta = 1$  and (b) on the ratio of the time step  $\Delta t$  and the average time between the two collisions  $t_1$  for rarefaction parameter  $\delta = 1$  ( $\square$ ) and  $\delta = 100$  ( $\circ$ )

allows using cells of larger size without loss in accuracy of simulations.

The dependence of the mass flow rate on the ratio of the time step  $\Delta t$  and the mean time between two collisions  $t_1$  for two very different values of the rarefaction parameters,  $\delta = 1$  and  $\delta = 100$ , is given in Fig. 2b. To eliminate the systematic error, we have to use a time step such that the ratio  $t_1/\Delta t$  stays approximately the same. Also, it is independent of the computation domain size  $L$ .

As mentioned above, a necessary condition for using the majorant frequency scheme is that each cell has to contain enough particles to make the number of collisions in it much greater than 1. However, our results show that this condition can be relaxed to a certain degree. In Fig. 3a, we show the mass flow rate dependence on the average number of collisions in a cell over a time step  $\Delta t$  for  $\delta = 1$  and  $L = 5h$ . We do not observe any systematic error related to having different numbers of particles in the cell even when the number of collisions over one time step is of the order of

1. Furthermore, additional analysis showed that this conclusion is independent of  $L$  and  $\delta$ . Therefore, in our simulations, we adhered the following guidelines: the number of collisions in each cell over a single time step has to be greater than 1 and each subcell has to contain at least 5–6 particles. Depending on the number of cells, the total number of particles varied in the range  $(5-25) \cdot 10^6$ .

The size of the computation domain also plays a very important role for reducing the systematic part of error. Figure 3b shows the dependence of the mass flow rate through the slit on the computational domain size in units of  $h$  for the rarefaction parameter  $\delta = 1$ . As we observe, the minimum size of the domain at which the systematic error becomes negligible is about  $L = 50h$ . At lower degrees of rarefaction, the domain size can be significantly smaller. For example, for  $\delta = 10$ , the value  $L = 30h$  is already large enough, and for  $\delta = 100$ , we have  $L = 20h$ .

Because all particles are in the upstream container at the beginning of simulations, some time has to pass

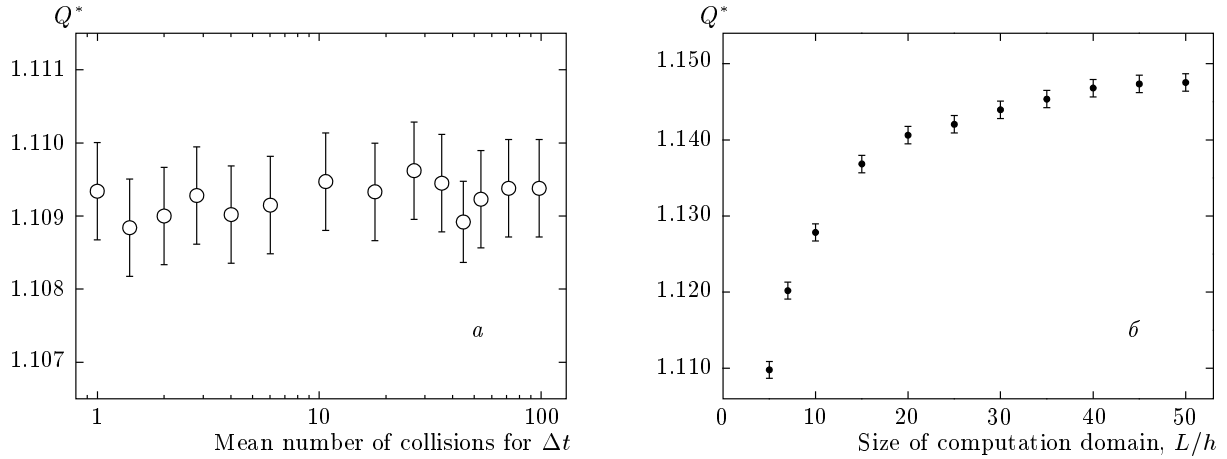


**Fig. 3.** The mass rate flow  $Q^*$  dependence on (a) the average number of the collisions in a single cell during one time step for  $\delta = 1$  and  $L = 5h$  and (b) on the relative size of the computation domain  $L/h$  for the rarefaction parameter  $\delta = 1$ , where  $h$  is the height of the slit

before a stationary flow regime is established. During this warm-up period, all obtained data are discarded, and only then we start collecting data on mass flow rate to obtain our estimates. As our simulations showed, the flow becomes stationary after times of the order of  $L/v_1$ . To be on the safe side, we extended the warm-up period to  $3L/v_1$ .

Because the results of simulations depend on the complete set of model parameters (in particular, as we have mentioned, the required cell size is different for different  $L$  and  $\delta$ ), we should be careful to make sure no systematic errors appear in each individual run. In other words, the set of model parameters should be chosen such that further improvement in the parameters (finer space grid, and so on) would not produce any improvement in the results at the level beyond the random part of the error.

Thus, the random part of simulations error can be decreased by running samples long enough, and the systematic part of error can be reduced to values of the order of or significantly less than the random error by choosing the model parameters appropriately. In our computations, the total error did not exceed 0.2%.

### 5. MAIN RESULTS

We used the model of hard spheres to simulate molecular collisions, and diffuse scattering to simulate interactions of gas molecules with the slit surface.

In Fig. 4, we show the results for the gas flow rate  $Q^*$  through a two-dimensional slit in the range of the rarefaction parameter  $\delta$  from 0.02 to 200. Solid sym-

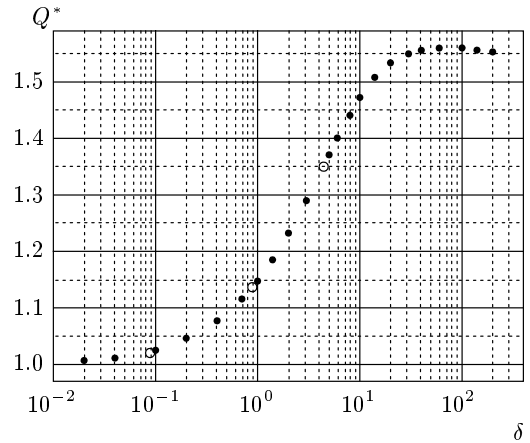


**Fig. 4.** The mass flow rate  $Q^*$  as a function of the rarefaction parameter  $\delta$ : solid symbols are our simulations; open symbols are the results in [10]

bols show our results and open symbols are the results obtained in [10] for the pressure ratio of the two containers equal to 50. We see that our results agree well with simulations in [10]. The results in [9] are noticeably lower, however. For example, the mass flow rate  $Q^*$  for  $\text{Kn}^{-1} = 1$  in [9] is about 1.10, and our result is 1.15. However, a much smaller computation domain was used in [9]. If we reduce the size of the domain from  $L/h = 50$  used in our simulations to  $L/h = 5$  used in [9], the mass flow rate also decreases to 1.10, as Fig. 3b shows.

As Fig. 4 shows, the mass flow rate increases very rapidly as the rarefaction parameter increases from 0.2

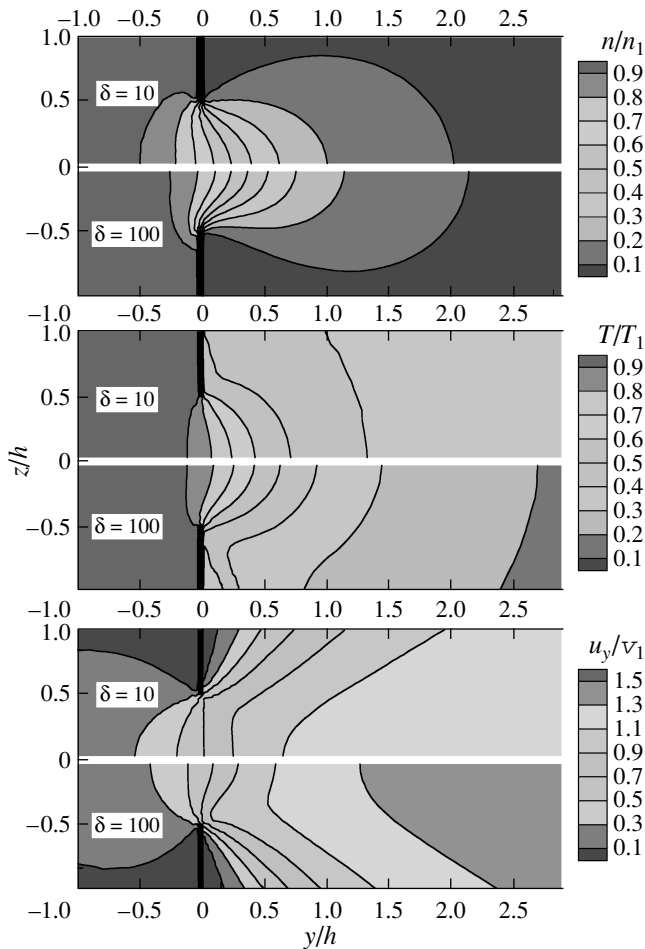


Fig. 5. The density  $n/n_1$ , temperature  $T/T_1$ , and lateral mass velocity  $u_y/v_1$  distributions near a slit in  $yz$  planes for  $\delta = 10$  and  $100$

to 20. At lower values of  $\delta$ , the dimensionless mass flow rate  $Q^*$  is close to the free molecular value given by (2) within 5%. As  $\delta$  increases beyond 20, the mass flow rate saturates very rapidly and approaches hydrodynamic limit (3).

The dimensionless gas density distribution  $n/n_1$ , where  $n_1 = P_1/kT_1$ , the temperature  $T/T_1$ , and the lateral component of the mass velocity  $u_y/v_1$  close to the slit in the  $yz$  plane for  $\delta = 10$  and  $\delta = 100$ , are presented in Fig. 5. For visual clarity, the bold lines in the figure indicate a part of the slit wall (although the slit is assumed infinitesimally thin). These distributions demonstrate that although macroscopic gas parameters change with the flow rate, qualitative characteristics of the flow field remain essentially the same.

In Fig. 6, we show the computed distributions of the

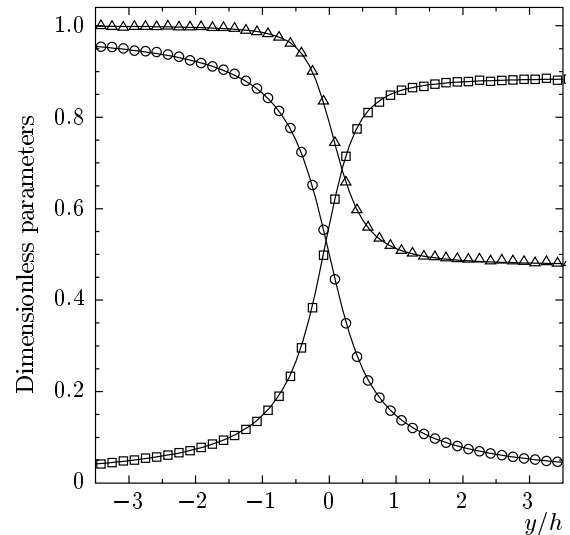


Fig. 6. Distribution of density  $n/n_1$  ( $\circ$ ), temperature  $T/T_1$  ( $\triangle$ ) and lateral mass velocity  $u_y/v_1$  ( $\square$ ) along the central line of the slit in free molecular regime and the corresponding analytic expressions [9] (solid lines)

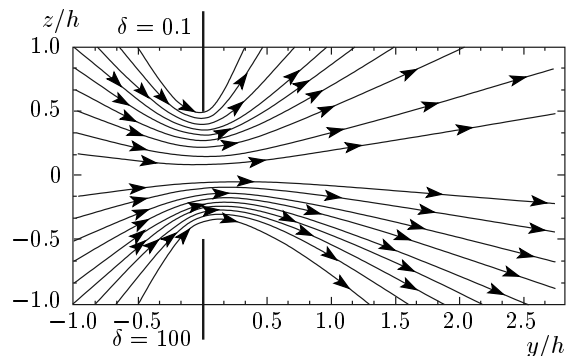


Fig. 7. Streamlines near the slit for  $\delta = 0.1$  and  $\delta = 100$

density, temperature and lateral mass velocity along the central line of the slit in the free molecular flow regime, along with the corresponding theoretical predictions in [9]. As we see, they agree quite well.

The streamlines on both sides of the slit for  $\delta = 0.1$  and  $\delta = 100$  are shown in Fig. 7. As we see, in a close-to-the-molecular flow regime (at  $\delta = 0.1$ ), streamlines are almost symmetric upstream and downstream. As  $\delta$  increases and gas becomes denser, the symmetry is lost.

## 6. CONCLUSIONS

To conclude, we have attempted to study gas flow into vacuum through an infinitesimally thin two-dimensional slit in a wide range of rarefactions using the direct simulation Monte Carlo method. The most significant change in the mass flow rate is observed in the rarefaction parameter range from 0.2 to 20. In the free molecular flow regime and in the hydrodynamic limit, our results agree with theoretical asymptotes [4, 6, 9], and in the transition regime, they compare well with numerical simulations by other authors [9, 10]. We also present the density, temperature, and lateral mass velocity distributions, as well as streamline analysis.

The next step would be to look at gas flow in channels of finite length and then in channels of complex geometry similar to MEMS/NEMS geometry. Also, it seems important to study the influence of the gas molecule–molecule interaction, gas–surface scattering, and finally to model effect of the surface structure and a finite ratio of the pressures in containers.

The Institute of Mathematics and Mechanics, Ural Branch of the Russian Academy of Sciences is acknowledged for computer facilities.

## REFERENCES

1. W. Steckelmacher, Rep. Prog. Phys. **49**, 1083 (1986).
2. M. R. Wang and Z. X. Li, Microfluid Nanofluid **1**, 62 (2004).
3. O. V. Sazhin, S. F. Borisov, and F. Sharipov, J. Vac. Sci. Technol. A **19**, 2499 (2001); Erratum **20**, 957 (2002).
4. F. Sharipov and V. Seleznev, J. Phys. Chem. Ref. Data **27**, 657 (1998).
5. G. A. Bird, *Molecular Gas Dynamics and the Direct Simulation of Gas Flow*, Oxford University Press, Oxford (1994).
6. H. W. Liepmann, J. Fluid. Mech. **10**, 65 (1961).
7. M. Hasegawa and Y. Sone, Phys. Fluids A **3**, 466 (1991).
8. C. Raju and J. Kurian, Exp. Fluids **17**, 220 (1994).
9. C. H. Chung, T. G. Keith, D. R. Jeng Jr., and K. J. De Witt, J. Thermophys. Heat Transfer. **6**, 27 (1992).
10. D. C. Wadsworth and D. A. Erwin, Phys. Fluids A **5**, 235 (1993).
11. M. S. Ivanov and S. V. Rogazinskiy, Mat. Model **1**, 130 (1989).
12. M. S. Ivanov and S. V. Rogazinskiy, Zh. Vychisl. Mat. Mat. Fiz. **28**, 1058 (1988).
13. M. S. Ivanov, private communication (2007).